

Radionuclides and stable elements in the sediments of the Yesa Reservoir, Central Spanish Pyrenees

Ana Navas · Blas Valero-Garcés · Leticia Gaspar · Leticia Palazón

Received: 13 April 2011 / Accepted: 15 July 2011 / Published online: 13 August 2011
© Springer-Verlag 2011

Abstract

Purpose The sediments accumulated in the Yesa Reservoir (Central Spanish Pyrenees) have greatly decreased its water storage capacity and are a major threat to the sustainability of water resources in the region. This study examines the contents of radionuclides and stable elements in the reservoir sediments and relates their variations with the sediment composition and local sedimentary dynamics, particularly flood frequency and intensity, which are responsible for changes in the main supply and distribution of radionuclides in the basin.

Materials and methods The sedimentary sequence accumulated in the Yesa Reservoir (471 Hm³), which supplies water to ca. 1,000,000 people and for irrigation, was examined in two 4-m long sediment cores (Y1, Y2) and one profile (Y3) retrieved at its central part. In the sediments, radionuclide activities of ²³⁸U, ²²⁶Ra, ²³²Th, ⁴⁰K, ²¹⁰Pb and ¹³⁷Cs were measured using a hyperpure Ge coaxial detector. The stable elements Mg, Ca, Sr, Ba, Cr, Cu, Mn, Fe, Al, Zn, Ni, Co, Pb, Li, K and Na were analysed by ICP-OES. Complementary analyses to characterize the sediments included: XRD in the profile, grain size distribution by laser equipment and the contents of organic matter, carbonates and the residual fraction by loss on ignition.

Results and discussion The variation in radionuclide activities is associated with grain size and sediment composition. The activity levels (becquerels per kilogram) ranged between 20 and 43 for ²³⁸U, 14 and 40 for ²²⁶Ra, 7 and 56 for ²¹⁰Pb, 19 and 46 for Th²³², 1 and 48 for ¹³⁷Cs and 185 and 610 for ⁴⁰K. Enriched activity levels are associated with clayey and silty layers, and depleted levels with sandy layers. The levels of radionuclides and trace elements were significantly lower in the cores than in the profile because of its higher silicate content and the influence of inflow of spring mineral-rich waters. The correlations among radionuclides, sediment components and stable elements provided evidence of a stronger influence of the dynamics of sediment supply by floods in the central areas closer to the main channel (cores) than in the littoral areas (profile).

Conclusions The radionuclide distributions were consistent with the history of the reservoir infilling and with the processes of transport and accumulation of sediments. Compared to the natural radionuclides, the artificial radionuclide ¹³⁷Cs varied the most and showed distinctive patterns. The methods used allowed the identification of natural inputs into the system and its differentiation from fluvial transport and reservoir deposition. The results provide insights into the pathways and processes involved in the mobilization of radionuclides in the environment.

Responsible editor: Ian Foster

A. Navas (✉) · L. Gaspar · L. Palazón
Department of Soil and Water, Estación Experimental de Aula Dei (EEAD-CSIC),
Apartado 13034,
50080 Zaragoza, Spain
e-mail: anavas@eead.csic.es

B. Valero-Garcés
Instituto Pirenaico de Ecología (IPE-CSIC),
Apartado 13034,
50080 Zaragoza, Spain

Keywords Gamma emitting · Natural and artificial radionuclides · Spanish Pyrenees · Stable elements · Sedimentary sequence · Siltation · Yesa Reservoir

1 Introduction

The sediments transported through a hydrological network and eventually accumulated in natural or human-made

water bodies can affect the quality and sustainability of water resources. Each year, about 1% of the capacity of the world's reservoirs is lost because of infilling by sediments, and this loss is a significant threat to the sustainability of water resources, not only in semi-arid areas but also at a global scale, considering that forecasted population growth will increase water demand.

Reservoirs act as sinks for radionuclides and stable elements, and, after being transported in dissolved or particle-associated forms, they remain trapped in different proportions in the sediment of reservoirs (McLean et al. 1991; Foster 2006). The accumulation of fallout ^{137}Cs and excess ^{210}Pb generally exceeds the atmospheric loadings, and estimates of their annual retention in three US reservoirs ranged between ~15% and ~80% (McCall et al. 1984). Moreover, radionuclides in the sediments deposited at the bottom of reservoirs might affect water quality for human consumption (Callender and Robbins 1993). Both artificial and natural radionuclides are also found in lakes (Morellón et al. 2008; Valero-Garcés et al. 2008), and their impact on natural ecosystem dynamics has to be evaluated. Therefore, the presence of radionuclides in the materials that accumulate in water bodies is an important environmental issue and requires an assessment of the mechanisms of radionuclide transport in fluvial networks and subsequent deposition in lakes and reservoirs.

The accumulation of sediments is a concern for most of the reservoirs in the Mediterranean region but, particularly, for those in mountainous areas, where high erosion rates and active sediment dynamics rapidly reduce the storage capacity of reservoirs. In 27 years, the Yesa Reservoir on the Aragón River, Spain, has lost 21 Hm^3 of its storage capacity (Centro de Estudios y Experimentaciones, CEDEX). Most of the sediments arrive via storm events and, to a lesser extent, via snowmelt (Navas et al. 2008). The sediment loads deposited in the Yesa Reservoir are expected to affect the sustainability of local water resources. Furthermore, a plan has been approved to double the initial water storage capacity of the reservoir, and, for that reason, the nature of the stored sediments contribute to the rational, sustainable use of water resources (Sundborg and Rapp 1986). Hence, the characterization of sediments accumulated in reservoirs is necessary for the implementation of sediment mitigating strategies. Moreover, data on radiological and stable elements provide more extensive information required for the application of environmental conservation policies of water bodies.

In the past century, soil erosion from agricultural catchments has increased the amount of sediment supplied to water courses, and changes in the sediment dynamics of catchments have been widely documented (e.g. Walling et al. 2003; Foster et al. 2007). In Mediterranean mountain headwaters, the impacts of land use changes have altered both runoff

generation and sediment transport in the recent decades (Navas et al. 2004), and thus, the transfer of natural and artificial radionuclides linked to soil particles might have also been affected. The analysis of the vertical distribution of radionuclides and stable elements in sedimentary records of reservoirs can assist with the identification of such changes. To improve the knowledge of the environmental behaviour of radionuclides and stable elements, more detailed information on specific processes in reservoirs is required. In addition, an understanding of stable elements and their association with the radionuclides is helpful in identifying their patterns of mobilization and any common sources of potentially toxic elements (Jordan et al. 1997).

The concentration profiles of radioisotopes and stable elements in sediment cores from reservoirs aid in the identification of natural inputs, environmental changes and artificial pollutants (Baeza et al. 2009). However, little is known about the radionuclide content and vertical distributions thereof, in the sediments of reservoirs in the Mediterranean region. In situ measurements should provide the ultimate information about the behaviour of radionuclide and stable elements of a particular ecosystem compartment such as reservoir deposits. This research examines the contents of radionuclides and other stable elements in the sediments that have accumulated at the bottom of the Yesa Reservoir (Aragón, Spain). The study based on a detailed analysis of the materials retrieved from two sediment cores and one profile collected from the submerged plains in the centre of the reservoir aims to provide insights into the pathways and the processes involved in the mobilization of the radionuclides in ecosystems. We also examined the relationships between the radionuclides and the general properties (e.g. grain size, organic matter, carbonates and silicate contents) of the sediments, the changes in sediment supply and the role of floods in the dynamics and transfer patterns of radionuclides and stable elements in Mediterranean mountain headwaters.

2 Materials and methods

2.1 The study area of the Yesa Reservoir

The Yesa Reservoir, located in the Aragón River (Fig. 1), in an E–W elongated valley carved in easily eroded Tertiary sedimentary formations, is one of the largest reservoirs in the Pyrenees (471 Hm^3) (see Fig. 1). The main inflow to the reservoir is supplied by the Aragón River (1,019 $\text{Hm}^3 \text{ year}^{-1}$). The reservoir was built in 1959 for irrigation of 60,700 ha and recently also supplies water to the Zaragoza metropolitan area with around 1,000,000 inhabitants.

The basin drained by the Aragón River has an altitudinal gradient varying between 570 and 2,900 m above mean sea

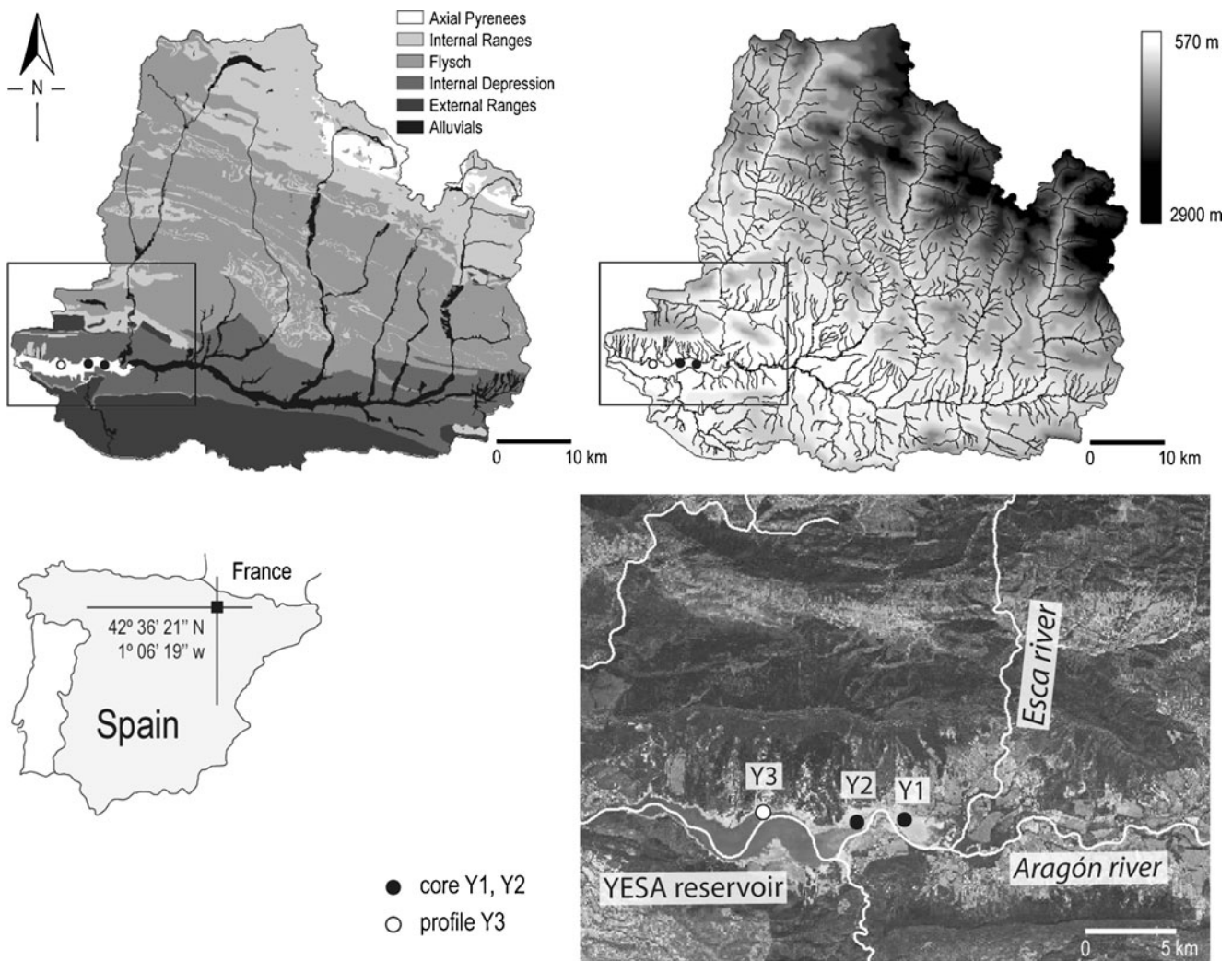


Fig. 1 The Yésa Reservoir: location of cores (Y1, Y2) and the profile (Y3) retrieved along the river axis. Lithological and geo-structural units and landscape of the basin of the Yésa Reservoir, Aragón, Spain

level, and upstream of the Yésa Reservoir covers an area of 2,191 km² with a diverse lithology consisting of: (a) magmatic and sedimentary Paleozoic rocks in the axial part, (b) calcareous Mesozoic rocks, Tertiary sandstones and marls of the Eocene Flysch in the Internal Ranges, (c) Eocene marls covered by Quaternary glacia and terraces in the Internal Depression and (d) conglomerates and sandstones in the Eocene–Oligocene External Ranges.

The Flysch is the predominant formation covering as much as 55% of the total surface. The main processes contributing to the supply of sediments and the siltation of the Yésa Reservoir are debris flows and slumps in the Axial and Internal Ranges (Lorente et al. 2002), intensive gully erosion on the marls at the Internal Depression and water erosion with abundant rills in the Flysch sector (Navas et al. 1997, 2005a).

The climate is transitional from temperate Atlantic to continental Mediterranean. Mean annual rainfall varies

between around 1,500 mm in the Internal Ranges and 800 mm in the Internal Depression. The distribution of natural vegetation follows an altitudinal pattern (Villar et al. 2001) from high mountain meadows, pine tree forest with some shrubs and the oak domain that was transformed into farmland in the last centuries.

In the reservoir, the main environments are the delta area at the mouth of the river, the submerged plains and the dam wall delta (Navas et al. 2008). The sedimentary sequence, established from cores that were retrieved from the submerged plains, comprises sediments accumulated >41 years since the dam was in full operation until the coring campaign, which were supplied mainly during floods (Navas et al. 2009). In this study, based on detailed sedimentological information that was linked with data on the hydrological regime, it was possible to distinguish three main periods of infilling. The first period, extending from the reservoir construction until 1979, had the highest flood frequency of the reservoir history

and was characterized by a succession of fining-upward sequences deposited successively in each flood. The second period (1979–1988) also registered a high sedimentation rate as result of the most intense floods for the whole studied period. The third period (1988–2000) had lower sedimentation coinciding with lower discharges and less frequent floods.

2.2 Core sampling and analyses

The radiological and geochemical characteristics of sediments accumulated in the reservoir were studied in two sediment cores (Y1 and Y2) and one sediment profile (Y3) that were collected along the reservoir axis at the submerged central plains (see Fig. 1). This part of the reservoir is considered the most stable and suitable environment to obtain a representative record of the materials accumulated in the bottom of the reservoir (Valero-Garcés et al. 1999; Navas et al. 2004).

At site Y3, the sedimentary profile (400 cm) was sampled during a survey carried out when the water level at the reservoir was very low and the meandering channel of the Aragón River was exposed. A section from the base to the top of the profile was hand-excavated, and samples of fresh sediment were collected at different depth intervals. The cores Y1 and Y2 were retrieved using a hand-operated, modified Livingstone corer. The length of the cores was 450 cm for core Y1 and 425 cm for core Y2. When the submerged plains were exposed, it was estimated that the total thickness of the deposit at the core sites reached 5.5–6.5 m; however, this total depth was not attained in the cores.

The sediment sampling considered the differences in the sedimentary record associated with different floods. The changes in sediment composition and grain size that were previously identified based on analyses performed on alternate 1-cm samples served to discriminate sedimentological facies in the sequence (Navas et al. 2009). Thus, sampling intervals were established after consideration of such differences in order to ascribe the radiological and geochemical properties to specific layers corresponding to different events.

The cores were split in half by using a cutter and a thin metal wire. A total of 21 and 13 samples were selected in cores Y1 and Y2, respectively, and 18 samples in profile Y3. Samples were placed in plastic bags for storage and kept refrigerated for laboratory processing and analysis. They were air dried and weighted following standard procedures. For the selected sample intervals, grain size, general composition, radionuclides and stable elements were analysed, as well as mineralogy for profile Y3. The results represented in the figures (described below) correspond to the middle of the sampled interval.

Grain size analysis of different size fractions was undertaken using laser equipment after particles were

stirred, chemically disaggregated and ultrasonically dispersed. The composition of sediments, organic matter and carbonate content and the residual fraction (mostly silicates) were measured by loss on ignition. The analysis of the total elemental composition was carried out after total acid digestion with HF (48%) in a microwave oven. Samples were analysed for the following 17 elements: Li, K, Na (alkaline), Mg, Ca, Sr, Ba (light metals) and Cr, Cu, Mn, Fe, Al, Zn, Ni, Co, Cd and Pb (heavy metals). Analyses were performed by atomic emission spectrometry using an ICP-OES (solid state detector). Concentrations, obtained after three measurements per element, are expressed in milligrams per kilogram.

In profile Y3, the mineralogical composition was determined by means of X-ray diffraction using a diffractometer equipped with a Si–Li detector using Cu K α radiation on random powders of bulk samples. The <2- μ m fraction was studied on oriented samples after standard treatment. The reflecting powers of Schultz (1964) for bulk samples were used for the quantitative estimation of the identified minerals.

Radionuclide activity in the samples was measured using a high-resolution, low-background, low-energy, hyperpure coaxial gamma-ray detector coupled to an amplifier and multichannel analyser. The detector had a 20% efficiency, 1.86 keV resolution (shielded to reduce background), and was calibrated using standard samples that had the same geometry as the measured samples. Subsamples of 50 g were loaded into plastic containers. Count times over 24 h provided an analytical precision of about $\pm 5\%$ to $\pm 15\%$ at the 95% level of confidence. Activities were expressed as becquerels per kilogram dry soil.

Gamma emissions of ^{238}U , ^{226}Ra , ^{232}Th , ^{40}K , ^{210}Pb and ^{137}Cs (in becquerels per kilogram air-dry soil) were measured in the bulk sediment samples. ^{238}U was not analysed in profile Y3. Considering the appropriate corrections for laboratory background, ^{238}U was determined from the 63-keV line of ^{234}Th , the activity of ^{226}Ra was determined from the 352-keV line of ^{214}Pb , ^{210}Pb activity was determined from the 47-keV photopeak, ^{40}K was determined from the 1,461-keV photopeak, ^{232}Th was estimated using the 911-keV photopeak of ^{228}Ac and ^{137}Cs activity was determined from the 661.6-keV photopeak.

3 Results and discussion

In the Yesa Reservoir, the sediments that have accumulated on the submerged plains are mostly silt (median range between 63% and 73%), with much smaller proportions of clay (16–23%) and sand (8–13%) (Table 1). Although the Y1 core had comparatively less sand and the Y2 core had comparatively more clay, the distribution of grain sizes was

Table 1 Basic statistics of the distribution of the grain size fractions, organic matter and the general composition of the sediments accumulated in the bottom of the Yesa reservoir

	%	Clay	Silt	Sand	OM	CO ₃ ⁼	Residual
Core Y1	<i>n</i> =21						
	Mean	17.9	67.3	14.8	3.7	42.0	54.4
	SD	4.8	12.9	16.5	0.9	8.4	8.3
	Min	9.0	28.0	2.0	2.0	23.0	34.0
	Max	29.0	77.0	63.0	5.0	64.0	75.0
Core Y2	<i>n</i> =13						
	Mean	21.2	57.4	21.4	3.3	38.5	58.2
	SD	6.6	14.4	20.1	0.8	4.3	4.1
	Min	8.0	20.0	6.0	2.0	30.0	51.0
	Max	31.0	70.0	72.0	4.0	45.0	66.0
Profile Y3	<i>n</i> =18						
	Mean	16.1	66.7	17.2	2.8	17.7	79.5
	SD	5.8	10.1	15.2	0.4	0.9	0.6
	Min	9.1	47.7	0.4	2.0	16.2	78.6
	Max	26.7	77.6	43.2	3.5	19.2	80.7

SD standard deviation

quite similar in the sediments at the three sampling sites. The percentage of the sedimentological facies as assessed by grain size, colour and sediment composition indicated that sandy and silty layers were most abundant in the profile (Y3), where they represented 90% of the total sedimentary record, whereas clayey and silty-clay layers predominated in the cores with the highest percentage in the Y2 core (82%).

Silicates and carbonates were the main components of the sediments which had homogeneous vertical distributions, and the amounts of organic matter were small (median range=2.8–4.0%). In the profile, the median of the residual fraction, i.e. silicates, accounted for as much as 80% and was, on average, 20% higher in the profile than it was in the two cores. Carbonates constituted ~40% of the cores but only 18% of the profile. In the cores, the distribution of the silicate and carbonate components varied little with depth.

The differences between the profile, which indicated a predominance of silicates and the abundance of sandy layers, compared to the two cores, which revealed a substantial carbonate component and an abundance of the finest fractions, might have resulted from the location of the profile, which was at the thalweg of the river channel. That location favoured the delivery of sandy materials into the inner parts of the reservoir. In addition, the greater energetic relief and the inflow from gullies near the site of the profile might have contributed to the high abundance of coarse materials in the profile. The mineral composition of the profile (*n*=18 samples) was calcite (39%), quartz (28%), clays (26%), plagioclase (4%), dolomite (2%) and feldspars (1%).

In the sediment of the cores and the profile, radioisotope activities were 20–43 Bq kg⁻¹ for ²³⁸U, 14–40 Bq kg⁻¹ for ²⁶Ra, 7–56 Bq kg⁻¹ for ²¹⁰Pb, 19–46 Bq kg⁻¹ for ²³²Th, 1–48 Bq kg⁻¹ for ¹³⁷Cs and 185–610 Bq kg⁻¹ for ⁴⁰K.

Those levels are similar to those found in the soils of the Flysch formation in the Yesa Basin (Navas et al. 2005b) where ¹³⁷Cs accumulates in the top layers while natural radionuclides are more homogeneously distributed in the soil profile. In sandstones, the normal concentrations of U and Th are 0.5–2.0 and 1–7 ppm, respectively, and in limestones, U and Th concentrations are ~2 ppm (Faure 1986). In the Yesa Basin, sandstones and limestones are the most abundant lithologies. Typically, in sedimentary rocks that have homogeneous mineral compositions, such as the marls and sand materials in the main formations of the Yesa Basin, radionuclide concentrations are constant (Faure 1986). Of the radionuclides detected in the Yesa Reservoir, ⁴⁰K had the highest activity levels. In the sediments that accumulated in an ancient Roman reservoir in southwestern Spain, ⁴⁰K also exhibited the highest activity (Baeza et al. 2009). Among the cores and the profile collected in the Yesa Reservoir, the vertical distributions of the artificial radionuclide ¹³⁷Cs and, to a less extent, ²¹⁰Pb and ⁴⁰K were highly variable; the levels of ²²⁶Ra and ²³²Th were the least variable and had the most homogeneous vertical distributions. The radionuclide activities were within the range of the background levels of the natural gamma radionuclides in the soils of a Flysch catchment, which is the formation that covers the most area in the Yesa Basin (Navas et al. 2011). In addition, activity levels were within the ranges found in surface formations in North America (de Jong et al. 1994; Litaor 1995) and Germany (Fujiyoshi and Sawamura 2004), but were less than the levels of ²³⁸U, ²²⁶Ra, ²³²Th, ⁴⁰K and ²¹⁰Pb detected in the sediments of the ancient Roman Proserpina Reservoir in southwestern Spain (Baeza et al. 2009). Those high activity levels are attributed to the geological environment of the reservoir, which is

within the Hesperic Spanish Massif, and consists of metamorphic rocks that have levels of radionuclides that are higher than those in the sedimentary rocks that predominate in the basin of the Yésa Reservoir.

In the two cores from the Yésa Reservoir, most of the radionuclide activities were quite similar, but they differed from those found in the profile (Fig. 2). The levels of ^{226}Ra , ^{232}Th , ^{210}Pb and ^{137}Cs were significantly higher in the profile than they were in the two cores, as indicated by an ANOVA (Table 2), probably because of the high silicate content of the former and the inflow of mineral-rich waters from Tiermas, a thermal source near the site where the profile was collected. With the exception of ^{210}Pb and ^{137}Cs , the lowest levels of radionuclides were in the Y1 core, which was located near the inflow from the Aragón River.

The high levels of ^{137}Cs might have been related to the supply of sediments from the gullies that reach the area near the site of the profile, which are likely to transport eroded soil that contains high levels of ^{137}Cs . Increasing mean values of ^{226}Ra were found following the submerged canal of the Aragón River. The two cores and the profile differed significantly in the levels of ^{226}Ra which was lowest at the site near where the Aragón River flows into the reservoir (core Y1) and highest in the profile (see Table 2) because the profile has a higher silicate content than the cores.

The activity levels of ^{238}U in the Y2 core were significantly lower than the levels in the Y1 core. ^{238}U and ^{226}Ra , which belong to the U series, differ greatly in their solubility, which affects their mobility, and ^{238}U is mobilized in the form of uranyl complexes (MacKenzie 2000). The activity levels of ^{40}K appeared to be directly associated with the mineralogy of the sediments. The level of ^{40}K was highest in the Y2 core, which likely resulted from the abundance of clayey layers and clay fractions in this core.

In the profile, the levels of the natural radionuclides were significantly positively correlated, which suggests that they had a common source (Table 3). In addition, the correla-

tions between the radionuclides were stronger and more likely to be statistically significant in the profile than they were in the cores. The low correlation between ^{210}Pb and ^{226}Ra in the cores is due to disequilibrium between the radionuclides (Krishnaswami et al. 1975; Bacon et al. 1976) caused by differences in the processes of geochemical differentiation (Benninger et al. 1975; Fleischer 1983). Preferential mobilization and scavenging by particulate material is also described for the removal of ^{210}Pb in the water–sediment interphase (Chi-Ju et al. 2004). This process is favoured in porous and fissured materials and depends on the particulate size (Mercer 1976), which agrees with our results that also suggest that this disequilibrium preferentially occurs in sand and silt materials.

In the Y2 core, the only significant correlations were between ^{226}Ra , ^{40}K and ^{232}Th . It is suggested that the sediments in the profile were mainly contributed from the surface soil containing high ^{137}Cs and silicate minerals with high natural radionuclides, while subsoils containing no ^{137}Cs and high carbonate minerals contributed to the sediments in the cores.

In the profile, the activities of ^{210}Pb , ^{226}Ra , ^{232}Th and ^{40}K tended to be positively correlated with the contents of the finest grain size fractions, but the opposite occurs with sand (Table 4). The strong positive correlation between the activities of ^{40}K and clay content reflects the tendency for this radionuclide to be associated with clay minerals because radioisotopes can adsorb to clay surfaces or become fixed within the lattice structure (Jasinska et al. 1982; Vanden Bygaart and Protz 1995). In the two cores, however, the correlations between radionuclides and sediment components were not as strong and less likely to be statistically significant. In the Y1 core, the amounts of organic matter and silicate materials of the residual fraction were significantly positively correlated with the abundance of each of the radionuclides, but the opposite was true for the relationships between carbonate content and the levels of the radionuclides. By comparison, in the cores, particularly Y2, the correlations between the levels of the radionuclides and the amounts of organic matter, silicates, carbonates and grain size fractions were weaker and less likely to be statistically significant. In the cores, the radionuclides transported with the sediments were more likely to be affected by changes in the hydrological regime than were those in the profile, which was from a site where changes in the supply of radionuclides can be masked by the local input of radionuclides from the thermal source of Tiermas.

3.1 Relationships between the radionuclides and stable elements

In the profile and the cores from the Yésa Reservoir (Table 5), Ca, Al and Fe (in that order) were the most abundant

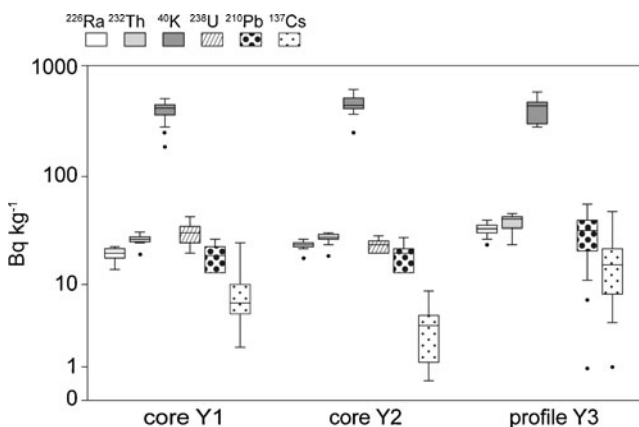


Fig. 2 Box plots of the radionuclide activity levels in the sediments of the Yésa Reservoir, corresponding to cores Y1, Y2 and profile Y3

Table 2 Basic statistics of the activity levels for the radionuclides assayed in the cores Y1, Y2 and profile Y3 retrieved from the sediments accumulated in the submerged plains of the Yésa Reservoir

		^{210}Pb Bq kg ⁻¹		^{226}Ra		^{137}Cs		^{40}K		^{232}Th		^{238}U	
Core Y1	<i>n</i> =21												
	Mean	18.9	a	19.5	a	8.3	a	394.8	a	26.9	a	30.4	a
	SD	5.0		2.6		5.5		79.5		3.2		6.7	
	CV%	26.7		13.5		66.4		20.2		11.8		21.9	
Core Y2	<i>n</i> =13												
	Mean	19.3	a	23.7	b	3.7	a	444.2	a	27.6	a	23.5	b
	SD	5.3		2.1		2.8		87.0		3.2		3.5	
	CV%	27.6		8.9		76.2		19.6		11.7		15.0	
Profile Y3	<i>n</i> =18												
	Mean	31.2	b	32.9	c	17.6	b	410.3	a	37.8	b	nd	
	SD	14.2		3.8		12.4		95.0		6.6		nd	
	CV%	45.5		11.7		70.4		23.1		17.6		nd	

Different letters indicate significant differences at the 95% confidence level

SD standard deviation, nd no data

elements, and K, Na and Mg were also present in significant amounts. Barium, Mn, Sr and Li were less common, and the concentrations of the heavy metals Zn, Pb, Cr, Ni, Cu, Co and Cd were low. The concentrations of the major and trace elements were within the ranges found in the soils in the Yésa Basin (Navas and Machín 2002) and those found in soils developed on similar parent materials (Kabata-Pendias and Pendias 2001).

In the profile, the Na content was higher, and Ca content was lower than in the cores; however, contents of Pb in the cores were nearly three times higher than the content in the profile. Typically, Pb is associated with clay minerals (Norris 1975). The content of Zn was higher in the Y2 core than it was in the profile and the Y1 core. Similarly to Pb, Zn is generally

associated with clay minerals, and the highest abundance of the clay fraction was found in the Y2 core. The contents of Ba and Mn and, to a lesser extent, Sr were higher in the Y2 core. Typically, Ba, Mn and Sr are associated with feldspars (Kabata-Pendias and Pendias 2001), which likely are contained in the most abundant clay size fraction in the Y2 core. Thus, the elements that are associated with clay and feldspar minerals and were most abundant in the cores appeared to be associated with the abundance of clayey layers in the cores.

The cores and the profile differed most significantly in the amounts of trace elements. The contents of Cr, Ni, Cu and Co in the profile were ten times higher than the contents in the cores, and Cd occurred in the profile only. The high content of microelements in the profile likely was related to the thermal

Table 3 Pearson correlation coefficients between the radionuclide activities (becquerels per kilogram) in the sediments of the Yésa Reservoir assayed in the cores Y1, Y2 and profile Y3

Core Y1					
	^{210}Pb	^{226}Ra	^{137}Cs	^{40}K	^{232}Th
^{226}Ra	0.283				
^{137}Cs	-0.012	0.149			
^{40}K	0.589	0.572	0.427		
^{232}Th	0.500	0.769	0.284	0.710	
^{238}U	0.365	0.463	-0.005	0.444	0.420
Core Y2					
	^{210}Pb	^{226}Ra	^{137}Cs	^{40}K	^{232}Th
^{226}Ra	0.285				
^{137}Cs	-0.026	0.161			
^{40}K	0.113	0.693	0.356		
^{232}Th	0.162	0.781	0.325	0.652	
^{238}U	0.032	-0.374	0.111	0.041	-0.232
Profile Y3					
	^{210}Pb	^{226}Ra	^{137}Cs	^{40}K	
^{226}Ra	0.823				
^{137}Cs	0.642	0.686			
^{40}K	0.837	0.788	0.596		
^{232}Th	0.823	0.732	0.548	0.682	

Boldface numbers are significant at the 95% confidence level

Table 4 Pearson correlation coefficients between the radionuclide activities and the percentages of the grain size fractions and the general composition of the sediments in the cores Y1, Y2 and profile Y3 retrieved in the Yesa Reservoir

		Clay %	Silt	Sand	OM	CO ₃ ⁼	Residual
Core Y1	²¹⁰ Pb	0.200	0.365	-0.343	0.186	-0.296	0.276
	²²⁶ Ra	0.076	0.254	-0.221	0.571	-0.275	0.212
	¹³⁷ Cs	0.094	-0.021	-0.011	-0.500	-0.588	0.646
	⁴⁰ K	0.459	0.412	-0.455	0.097	-0.518	0.509
	²³² Th	0.170	0.503	-0.443	0.376	-0.466	0.425
	²³⁸ U	0.000	0.107	-0.083	0.156	0.123	-0.141
Core Y2	²¹⁰ Pb	0.315	0.512	-0.470	-0.296	0.341	-0.298
	²²⁶ Ra	0.535	0.529	-0.554	0.330	-0.587	0.546
	¹³⁷ Cs	0.227	0.124	-0.164	0.247	0.136	-0.186
	⁴⁰ K	0.784	0.579	-0.672	0.457	-0.430	0.361
	²³² Th	0.586	0.611	-0.630	0.568	-0.463	0.374
	²³⁸ U	0.217	-0.132	0.023	-0.467	0.210	-0.131
Profile Y3	²¹⁰ Pb	0.591	0.654	-0.662	0.740	-0.881	0.810
	²²⁶ Ra	0.642	0.637	-0.670	0.496	-0.757	0.792
	¹³⁷ Cs	0.313	0.174	-0.236	0.388	-0.487	0.462
	⁴⁰ K	0.876	0.742	-0.830	0.818	-0.920	0.813
	²³² Th	0.493	0.638	-0.614	0.557	-0.712	0.682

Boldface numbers are significant at the 95% confidence level

source of Tiermas that may supply substantial amounts of Cr, Ni, Cu, Co and, to lesser extent, Cd that came from the mineral-rich waters. In addition, the abundance of silicates in the sediment composition of the profile may also contribute to the high contents of radionuclides and trace elements because heavy metals and radionuclides are enhanced in argillaceous materials (Kabata-Pendias and Pendias 2001).

In the profile, among the direct and significant correlations, those between ²²⁶Ra, ²³²Th, ²¹⁰Pb, ⁴⁰K, with K and Mn, and between ²²⁶Ra, ²³²Th and ⁴⁰K with Cu and Cd (Table 6) suggest that these radionuclides and the stable elements were from a common source. However, the activities of fallout ¹³⁷Cs were not correlated with the stable element contents, which confirmed that this artificial radionuclide had a different source. In the Y1 core, some of the relationships between the radionuclides and the elements differed from those detected in the profile. The activities of most of the radionuclides were inversely correlated with the contents of Ca and Sr, which suggested the absence of a link with carbonates. Although the radionuclide activities were positively correlated with contents of Zn, Cr and Fe, the reverse was true in the profile. In the Y2 core, the relationships between radionuclides and stable elements were much less clear, and only a few correlations were statistically significant.

3.2 Vertical distribution of the ²³⁸U/²²⁶Ra and ²³²Th/²²⁶Ra activity ratios

The U and Th series are commonly associated in nature. Ivanovich (1994) reported a quasi-constant mass ratio of those decay series in natural systems, although this

equilibrium is often disturbed by physical and chemical processes that enhance a loss or gain of a given decay product. Thus, activity ratios between parent/parent or between progeny pairs can be used to assess the maintenance of the initial proportionality between the ²³²Th and ²³⁸U decay series. Furthermore, ²³⁸U/²²⁶Ra activity ratios can be used to ascertain equilibrium within the same decay series. If secular equilibrium prevails in the ²³⁸U chain, the activity ratios of ²³⁸U/²²⁶Ra will be approximately 1; therefore, values other than 1 indicate disequilibrium. In the sedimentary record of the Yesa Reservoir, most of the samples in the cores had ²³⁸U/²²⁶Ra ratios that were >1.0, which indicated disequilibrium in the ²³⁸U chain (Table 7). Ratios higher than 1 suggest ²³⁸U enrichment which might have been due to large differences in the mobility of these radionuclides (Dowdall and O'Dea 2002). Disequilibrium was greater in the Y1 core than it was in the Y2 core, and the greatest deviations from the linear trend occurred in the upper 200 cm of both cores, where sediments of fine grain size were most abundant. In addition, sorption is an important component of the U cycle (Kabata-Pendias and Pendias 2001), and significant accumulations of U are often associated with clays because the clay fraction has an affinity for absorbing U and Th (Megumi et al. 1982).

The ²³²Th/²²⁶Ra activity ratio (i.e. the progeny pair ²²⁸Ac/²¹⁴Pb) can be used to assess the maintenance of the proportionality within the ²³²Th and ²³⁸U decay series, which is about 1.1 in most environmental samples (Evans et al. 1997). In our study, most of the samples had ²³²Th/²²⁶Ra activity ratios that were >1.1, although the deviations from the original proportionality were less than they were for the

Table 5 Basic statistics of the contents of stable elements (milligrams per kilogram) analysed in the sediments of profile Y3 and cores Y1 and Y2 in the Yesa Reservoir

	Ca	Al	Fe	K	Na	Mg	Mn	Sr	Ba	Li	Pb	Zn	Cr	Ni	Cu	Co	Cd
Y1	Mean	100,894	22,588	17,643	10,436	4,920	3,567	392.9	229.7	73.8	85.2	50.7	5.0	1.8	1.6	1.6	bdl
	Median	101,110	22,878	18,604	10,907	4,684	3,594	402.4	179.1	74.8	86.8	51.5	5.3	1.8	1.4	1.6	bdl
	SD	13,270	4,079	2,449	2,072	1,350	616	42.3	131.5	8.5	11.6	8.5	1.1	0.4	0.5	0.2	bdl
	Min	72,437	10,866	11,450	4,493	3,528	2,088	263.6	57.2	50.0	51.0	26.1	2.0	1.0	1.1	1.1	bdl
	Max	130,565	31,392	20,374	14,090	9,718	4,885	406.5	594.6	85.7	108.9	61.3	6.3	2.9	2.7	1.9	bdl
Y2	Mean	105,266	25,086	18,244	9,781	6,943	3,815	436.7	479.2	84.9	81.1	65.3	4.5	2.5	1.6	0.5	bdl
	Median	104,179	26,035	18,006	9,592	6,923	3,638	410.6	366.4	89.0	82.5	53.0	4.4	2.6	1.8	0.6	bdl
	SD	13,175	2,976	2,238	1,912	1,045	532	68.3	284.0	10.9	9.9	33.0	1.0	0.5	0.4	0.2	bdl
	Min	83,922	18,834	14,236	6,276	4,797	3,156	365.5	246.6	66.4	57.9	37.7	2.8	1.6	0.9	0.1	bdl
	Max	130,543	28,930	22,423	12,681	9,175	4,812	598.4	1,082.1	99.1	92.9	139.5	6.0	3.3	2.1	0.7	bdl
Y3	Mean	89,239	26,161	18,144	10,661	9,554	4,007	375.7	216.9	82.3	33.9	52.3	56.9	26.6	14.7	9.9	1.9
	Median	90,700	25,900	17,800	10,600	9,505	3,880	376.0	257.5	81.0	34.7	52.8	58.6	26.4	13.8	10.4	1.4
	SD	9,281	3,089	2,183	1,750	1,372	657	28.8	34.8	9.4	6.8	8.3	9.9	3.8	4.6	1.6	2.1
	Min	70,600	18,900	14,900	7,730	7,180	2,700	296.0	166.0	67.7	16.3	41.2	42.2	20.6	12.0	6.6	0.8
	Max	105,000	31,300	22,100	13,400	13,100	5,170	411.0	279.0	94.1	43.2	63.6	69.3	31.0	32.1	12.1	10.0

SD standard deviation, *bdl* below detection level

$^{238}\text{U}/^{226}\text{Ra}$ ratio. In the profile, deviations from the linear trend were highest in the first 200 cm, but this was not observed in the cores, where the $^{232}\text{Th}/^{226}\text{Ra}$ activity ratio remained constant throughout the depth of the sedimentary record. Like ^{238}U , ^{232}Th can be easily mobilized in the form of organic compounds and various complex inorganic cations that can be absorbed by clays, which contributes to the differential mobility of ^{232}Th and ^{226}Ra .

3.3 The vertical distribution of radionuclides in the reservoir sediments

Variations in radionuclide activities with depth in the sedimentary sequence of the Yesa Reservoir might provide insights into the patterns and pathways of the terrestrial radioactivity (Fig. 3). In the profile, the activity levels were constant with depth, with the exception of a tendency for ^{137}Cs to be more prevalent and ^{232}Th to be more highly dispersed in the upper 200 cm of the profile. In the Y1 core, with the exception of ^{137}Cs , the levels of the radionuclides decreased slightly with depth, which appeared to be related to the predominance of sandy materials at the lower portion of the core. Similar to the profile, in the Y1 core, the activities of ^{226}Ra and ^{232}Th were the most constant during the infilling period, while the activities of ^{137}Cs varied the most and were highest in the deepest layers, which reflects temporal changes in its global fallout. The activities of ^{238}U were higher in the upper 200 cm than they were in the lower portion of the core. In the Y2 core, the pattern was not as clear because positive (^{226}Ra , ^{232}Th , ^{40}K) and negative (^{210}Pb , ^{137}Cs , ^{238}U) trends were apparent, which reflected increases and decreases in activity levels, respectively, with depth. In the Y2 core, with the exception of ^{210}Pb and ^{137}Cs , whose activities varied widely with depth, the radionuclides were distributed homogeneously, which indicated that their supply was constant throughout the infilling period, but this is also associated with low variation in the composition and the distribution of grain sizes in the sedimentary layers.

In general, for the entire sedimentary record in the reservoir, the more stable activities of ^{226}Ra and ^{232}Th reflect the almost constant contributions throughout the infilling period. The activities of ^{40}K and ^{210}Pb were more variable, but the greatest variation was in ^{137}Cs , which was a consequence of the pattern of its fallout, globally, and the close association between ^{137}Cs and the fine soil particles that are mobilized by physical processes such as erosion and delivered to the reservoir. The start of the operation of the reservoir in 1959 was almost coincidental with the onset of ^{137}Cs fallout, whose content has decreased with time (^{137}Cs half-life is 30.17 years) since fallout started in the 1950s until the early 1980s when its fallout essentially ceased; Chernobyl-derived ^{137}Cs fallout in the area was negligible.

Table 6 Pearson correlation coefficients between the radionuclide activities (becquerels per kilogram) and contents of stable elements (milligrams per kilogram) in the sediments of the Yesa Reservoir

	Mg	K	Na	Pb	Ba	Zn	Sr	Li	Mn	Co	Ni	Cu	Cr	Cd	Fe	Al	Ca	
Y1	²¹⁰ Pb	0.371	0.310	0.233	0.464	0.175	0.393	-0.056	0.446	0.278	0.441	0.349	0.342	0.345	0.080	0.204	0.465	-0.216
	²²⁶ Ra	0.443	0.668	-0.114	0.701	-0.189	0.635	-0.160	0.700	0.649	0.419	0.412	0.072	0.698	-0.070	0.652	0.653	-0.338
	¹³⁷ Cs	0.268	0.461	-0.349	0.149	-0.198	0.447	-0.625	0.341	0.334	0.116	0.474	0.002	0.323	-0.209	0.161	0.115	-0.690
	⁴⁰ K	0.603	0.877	-0.285	0.800	-0.118	0.908	-0.512	0.886	0.738	0.382	0.700	0.136	0.895	-0.286	0.765	0.718	-0.678
	²³² Th	0.536	0.702	0.067	0.720	0.082	0.694	-0.259	0.728	0.617	0.407	0.509	0.185	-0.088	0.536	0.698	-0.493	
	²³⁸ U	0.192	0.272	-0.228	0.242	0.019	0.394	-0.161	0.256	0.511	-0.036	0.268	0.278	-0.235	0.496	0.083	-0.288	
Y2	²¹⁰ Pb	-0.596	-0.003	0.314	-0.134	-0.230	0.572	-0.051	0.070	0.015	-0.111	-0.075	-0.119	0.008	0.126	-0.043	0.065	
	²²⁶ Ra	0.133	0.473	0.081	-0.006	0.296	0.412	-0.079	-0.192	0.471	-0.378	-0.042	-0.404	0.017	-0.415	0.139	-0.471	
	¹³⁷ Cs	0.331	0.079	0.065	0.032	0.443	-0.334	0.680	0.712	-0.493	0.660	0.625	0.643	0.465	0.687	0.145	0.211	0.268
	⁴⁰ K	0.443	0.714	-0.279	0.424	0.178	0.206	-0.060	0.221	0.468	-0.014	0.373	0.046	0.539	-0.152	0.364	0.531	-0.481
	²³² Th	0.252	0.558	-0.040	0.379	0.215	0.064	-0.113	0.172	0.316	0.008	0.312	0.039	0.430	-0.106	0.302	0.479	-0.545
	²³⁸ U	0.204	0.324	-0.233	0.422	0.006	-0.344	0.295	0.671	-0.142	0.604	0.640	0.503	0.501	0.484	0.277	0.284	0.048
Y3	²¹⁰ Pb	0.580	0.729	-0.374	0.394	-0.520	0.602	0.044	0.669	0.528	0.425	0.622	-0.209	-0.364	0.359	0.577	-0.519	
	²²⁶ Ra	0.674	0.695	-0.350	0.523	0.457	-0.469	0.540	0.122	0.630	0.453	0.454	0.568	-0.030	0.530	-0.270	0.376	0.660
	¹³⁷ Cs	0.439	0.401	-0.056	0.079	-0.047	-0.218	0.126	0.285	0.273	0.160	-0.073	0.195	-0.185	0.075	-0.229	-0.096	0.313
	⁴⁰ K	0.717	0.872	-0.301	0.689	0.481	-0.631	0.784	0.122	0.831	0.505	0.518	0.772	-0.130	0.738	-0.209	0.543	0.783
	²³² Th	0.492	0.687	-0.443	0.422	0.360	-0.419	0.502	0.035	0.607	0.577	0.387	0.553	-0.221	0.523	-0.390	0.338	0.475

Boldface numbers are significant at the 95% confidence level

Table 7 Basic statistics of the $^{238}\text{U}/^{226}\text{Ra}$ and $^{232}\text{Th}/^{226}\text{Ra}$ ratios in the cores Y1, Y2 and profile Y3 retrieved from the Yesa Reservoir

	Core Y1		Core Y2		Profile Y3
	$^{238}\text{U}/^{226}\text{Ra}$	$^{232}\text{Th}/^{226}\text{Ra}$	$^{238}\text{U}/^{226}\text{Ra}$	$^{232}\text{Th}/^{226}\text{Ra}$	$^{232}\text{Th}/^{226}\text{Ra}$
Mean	1.57	1.39	1.0	1.2	1.1
Median	1.59	1.39	0.96	1.17	1.17
SD	0.31	0.13	0.2	0.1	0.1
Min	1.00	1.22	0.7	1.0	0.8
Max	2.29	1.71	1.5	1.3	1.3

SD standard deviation

However, sediment age is unlikely to exert an important control on the activity levels of ^{137}Cs , compared to the intense sedimentary dynamic that deposited more than 6 m of sediments at the submerged plains of the reservoir.

In general, the activity levels of the radionuclides were lowest in the layers of the sediment that had predominantly coarse fractions; i.e. sandy layers had the least radionuclide content (Figs. 4, 5, 6). Conversely, the activity levels of the radionuclides were highest in the layers that were composed of clayey materials. In the Y1 core, collected near the point where the Aragón River flows into the reservoir, the radionuclide content was lowest at the bottom of the core in a thick layer of coarse grey sands, which indicated the occurrence of an extreme flood, and in a sandy layer 32.5 cm from the top of the core, which was deposited by another intense flood. The infilling of the Yesa Reservoir occurred as a succession of fining-upward sequences, each reflecting major flood episodes that have characteristic patterns of the frequency and intensity of floods which appear to be correlated with the activity levels of the radionuclides.

Features of the sedimentary record, such as the distribution of fining-up grain size sequences, the thickness and distribution of alternating layers, helped to identify the three deposition units that occurred during the period of infilling (Navas et al. 2009). Frequent, regular periods of floods in the period 1959–1979 were accompanied by the regular deposition of fining-up sequences. In the period 1979–1988, there were fewer floods. In the period 1988–2000, floods were less intense, but occurred more frequently than they did in the previous period, which was paralleled by less energetic silty fining-upward sequences. Consequently, radionuclide activity levels in the sandy layers that marked the beginning of a flood were low. The levels of ^{137}Cs were highest in the lower section of the Y1 core (depth=336–392 cm) and were associated with clayey layers. In a reservoir on the Loess Plateau, China, ^{137}Cs concentrations were highest in the finest sediments of the infilling sequences caused by floods (Zhang et al. 2006). The radioisotopes ^{137}Cs and unsupported ^{210}Pb can be used to discriminate sources of reservoir sediments (e.g. Foster et al. 2007; Simms et al. 2008).

In the Yesa Reservoir, sandy material was most abundant (almost 25%) in the core (Y1) that was collected near the

entrance of the Aragón River. Clayey and silty-clay layers were more predominant (82%) in the Y2 core than in the Y1 core (40%) which is the main reason why the variations in radionuclide activity levels were not as marked in the former as they were in the latter. The more marked pattern in the variation of the radionuclides in the profile resulted from the high frequency of alternations between sandy and clayey layers. The highest activity levels of all of the natural radionuclides occurred at depths of 200, 255, and 365 cm, which coincided with the period of the highest frequency of intense floods occurring in the lower part of the profile and the predominance of less frequent and less energetic floods in the upper part of the sedimentary record. In addition, the highest levels of ^{137}Cs occurred in the profile between 200 and 225 cm, which coincided with periods of frequent, high-intensity floods, which would have triggered intense erosion in the Yesa Basin. In general, ^{137}Cs content decreased in the upper part of the cores and the profile. ^{137}Cs remains strongly fixed to the fine soil fractions and has little mobility; thus, it would have been transported with eroded materials. In a reservoir on the Danube River which had a predominance of silty sediments, ^{137}Cs was concentrated in <20- μm fractions of organic material, clays and Fe and Mn oxides. Furthermore, the radionuclides varied little, and activity levels also increased with decreasing grain size (Rank et al. 1987).

In the profile, all of the radionuclides showed quite similar depth distributions, although ^{226}Ra and ^{232}Th , the least mobile of the radioisotopes, did not exhibit marked peaks in activity. The depths at which the maximum levels of radioisotope activity occurred were similar in the Y1 core and the profile, which suggests that the transport of the radionuclides through the reservoir occurred during the same floods and that the distribution of radionuclides was the same near the entrance as it was in the inner section of the reservoir. Furthermore, the local input of radionuclides identified in the profile, which were associated with the thermal sources at Tiermas, adds to the content of radionuclides transported with the sediments.

Differences in the frequency, intensity and occurrence of floods and the variations in the hydrological regime led to

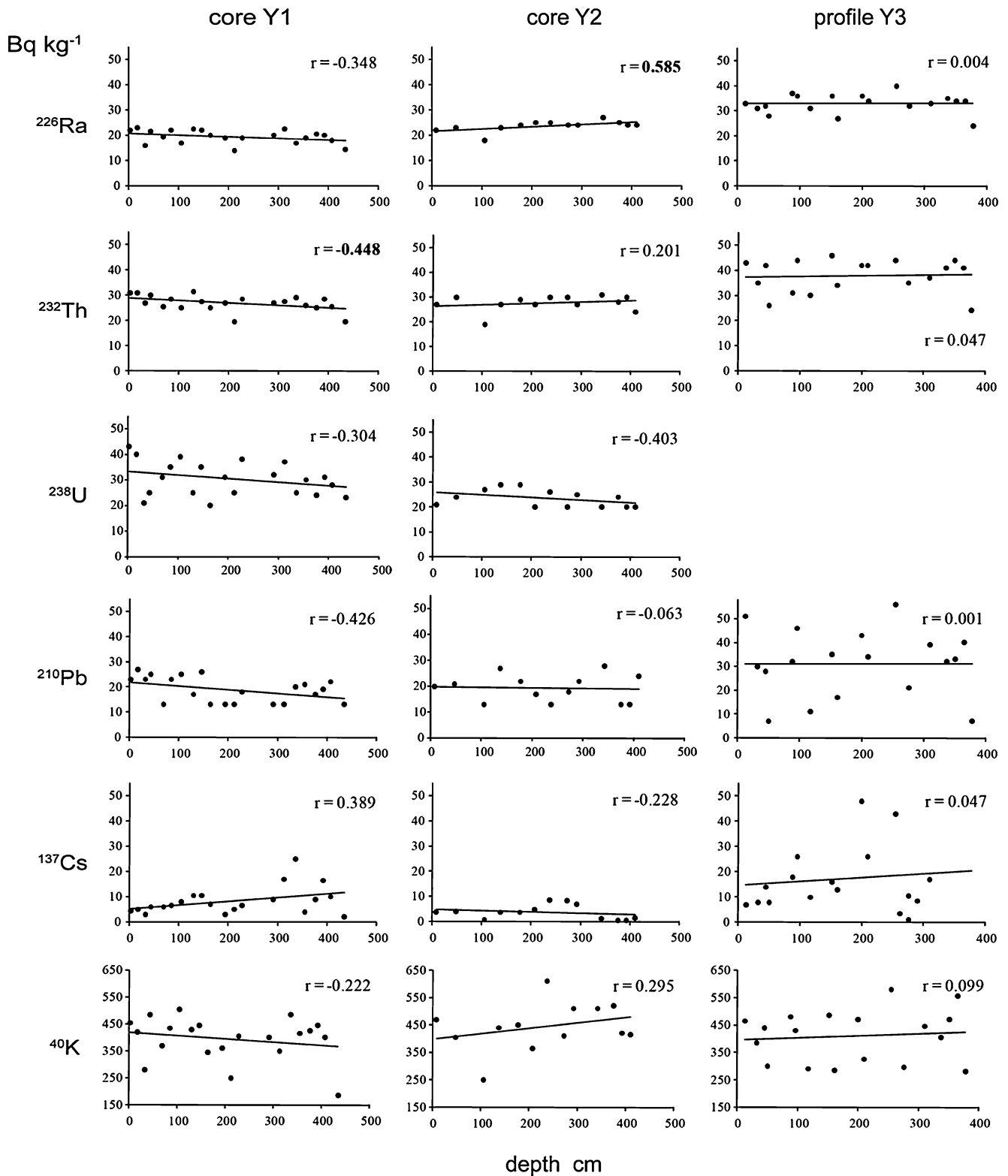
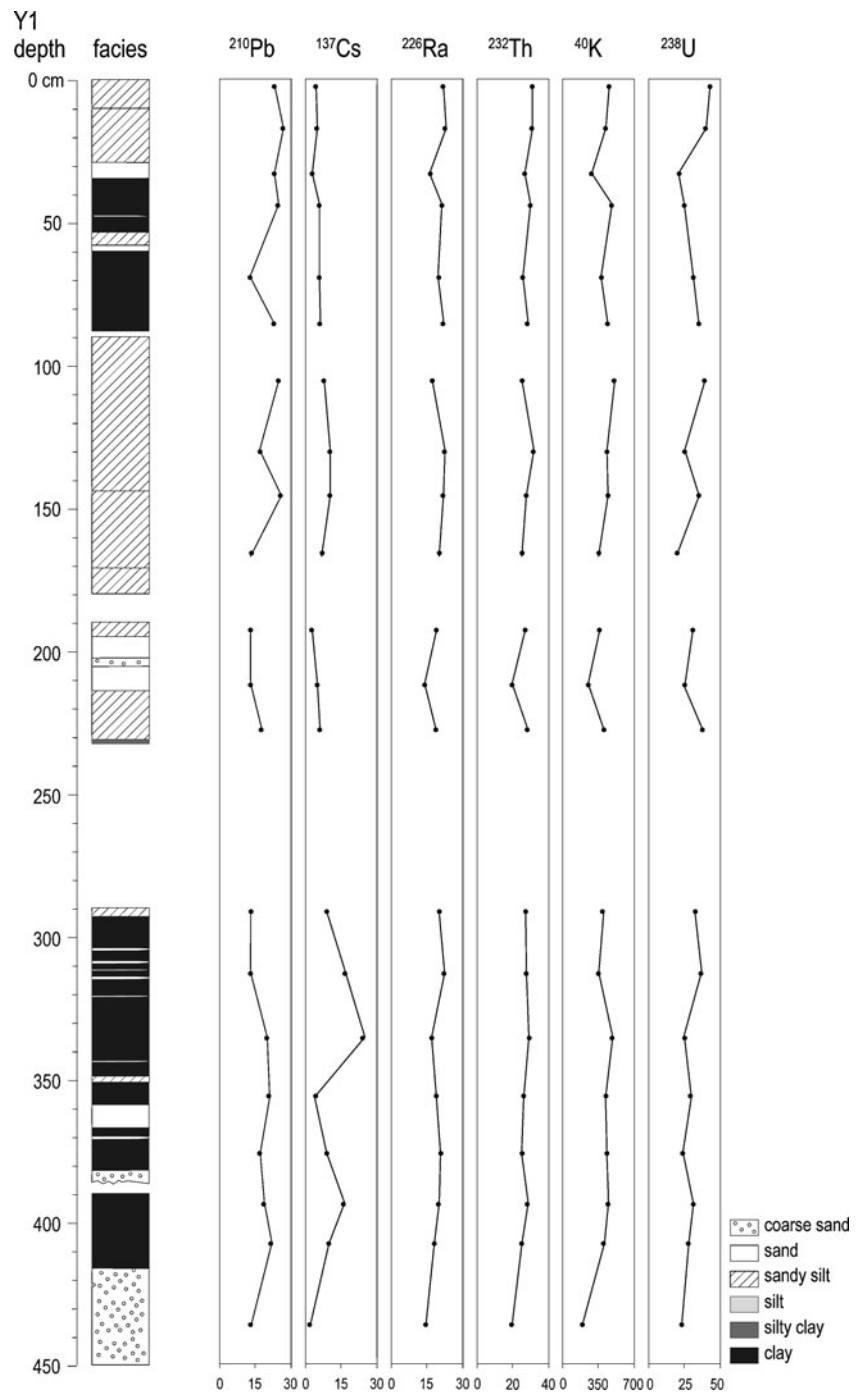


Fig. 3 Variations of radionuclide activities with depth in the cores Y1, Y2 and profile Y3 of the Yesa Reservoir

differences in the characteristics of the sediments. Furthermore, those differences appear to have affected the distribution of radionuclides. The activity levels of the natural radionuclides

were highest at the lower part of the sedimentary record, which coincides with an energetic fluvial regime that caused the highest sedimentation rates in the reservoir (Navas et al. 2009).

Fig. 4 Vertical distribution of the radionuclides (becquerels per kilogram) in the sedimentological facies identified in core Y1 taken in the submerged plains of the Yesa Reservoir

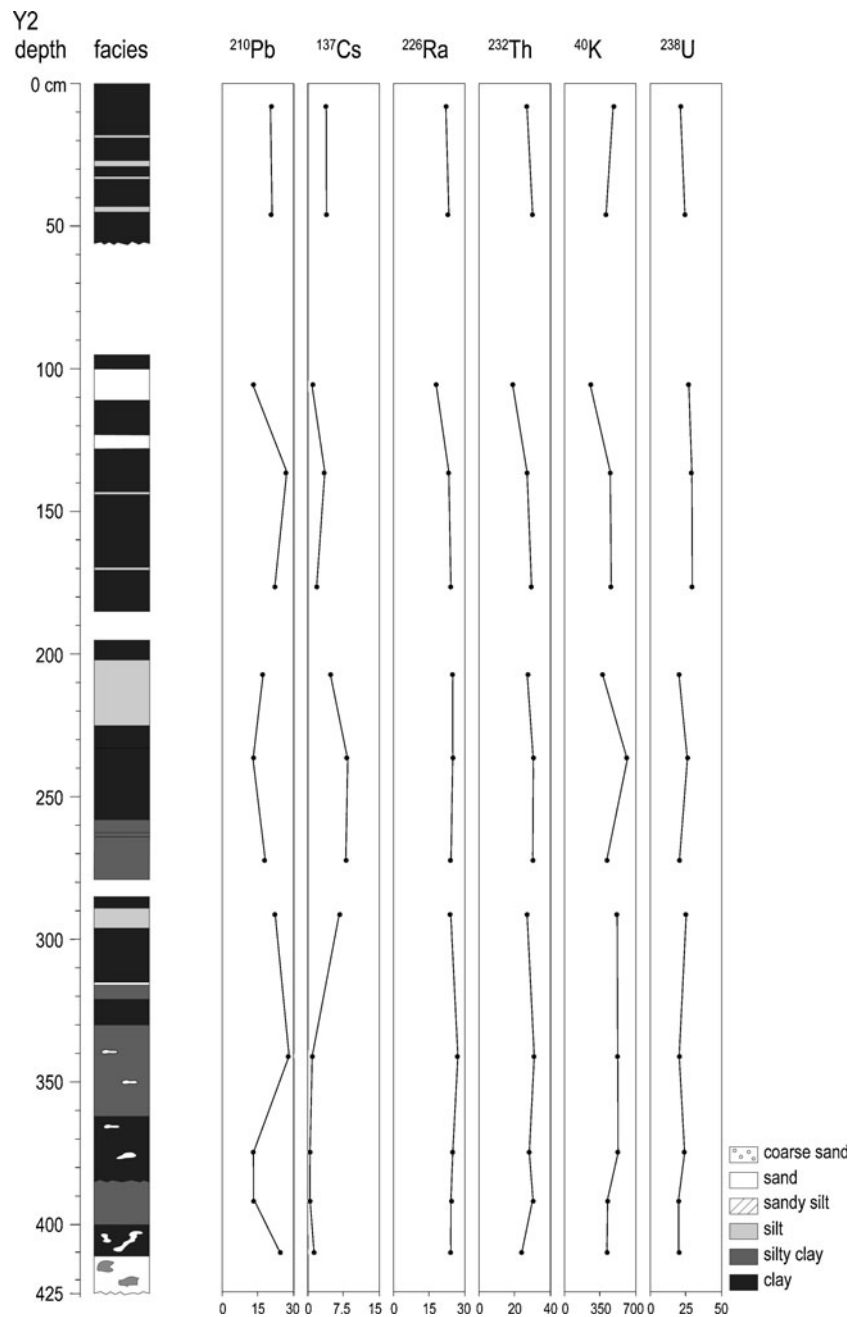


4 Conclusions

In the last half century, the infilling of the Yesa Reservoir in Spain produced variable sedimentological characteristics that were attributed to variations in the hydrological regime of the Aragón River and its tributaries that drained the catchment, which, in turn, has affected the distribution of radionuclides within the sedimentary sequence.

In the Yesa Reservoir, the sediments which arrive mainly during floods and, subsequently, are redistributed in ways that are influenced by the water level in the reservoir had radionuclide levels that are within the range observed in similar environments. Variations in radionuclide activities are associated with the grain size and composition of the accumulated sediments. Enriched activity levels are associated with clayey and silty layers, and depleted levels are

Fig. 5 Vertical distribution of the radionuclides (becquerels per kilogram) in the sedimentological facies identified in core Y2 taken in the submerged plains of the Yesa Reservoir



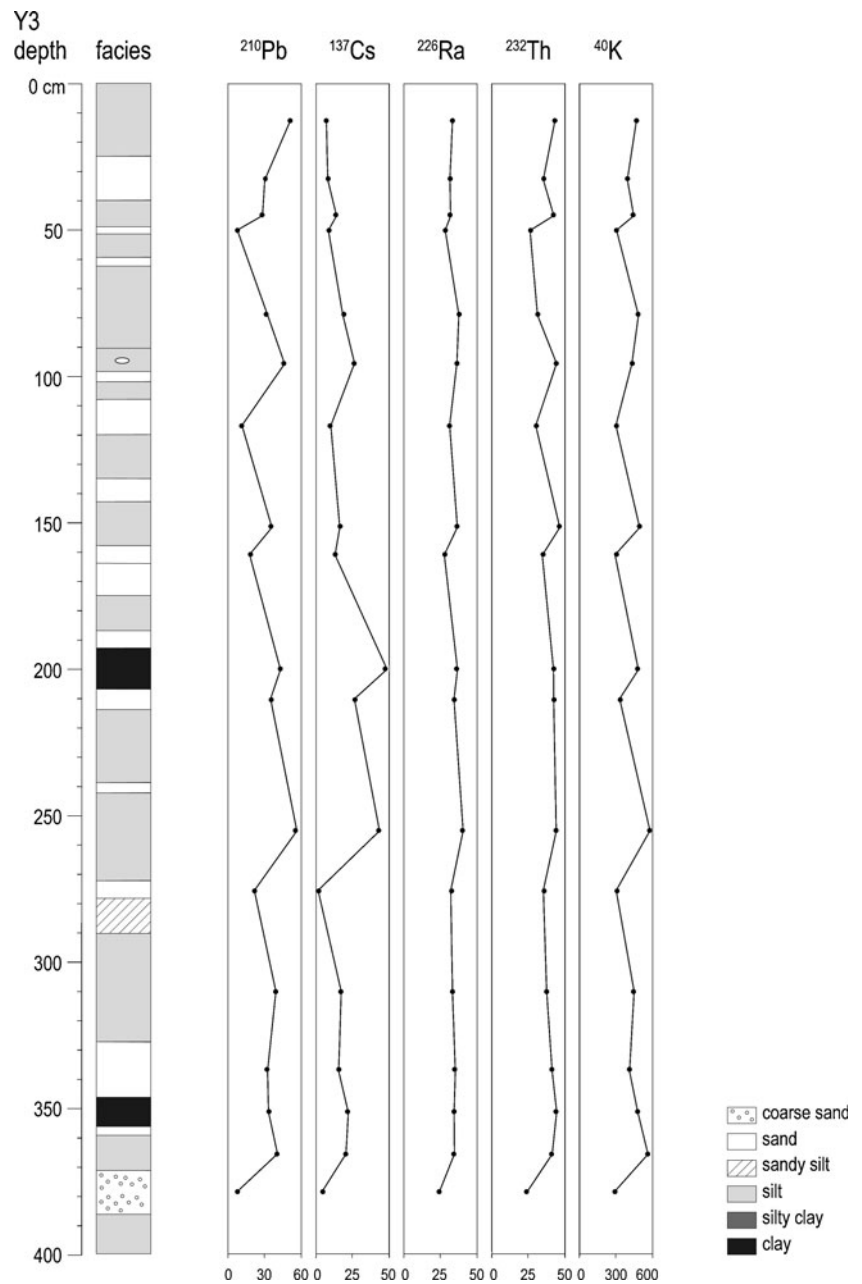
associated with sandy layers that have predominantly coarse fractions. Clearly, sedimentological processes influence the patterns of radionuclide accumulation. The distributions of the radionuclides were consistent with the history of the infilling of the reservoir and with the processes of transport and the accumulation of sediments.

The levels of radionuclides and stable elements were higher in silicate-rich sediments such as those in the profile

compared to those in the cores. Enhanced levels of radionuclides and some stable elements were associated with the mineral-rich thermal source of Tiermas, which is near the site where the profile was collected.

The sedimentary record in the Yesa Reservoir provided an opportunity to quantify the abundance and distribution of radionuclides within the reservoir–catchment system, which is important to compare with environmental baselines in order to

Fig. 6 Vertical distribution of the radionuclides (becquerels per kilogram) in the sedimentological facies identified in the profile collected from the submerged plains within the Yesa Reservoir



preserve the quality of water bodies. The methods used in this study provided information that permitted an assessment of the patterns of accumulation of radionuclides in reservoir sediments and allowed the identification of natural inputs into the system and its differentiation from inputs associated with fluvial transport and reservoir deposition.

Assessments of the radionuclides that are contained in the sedimentary records of reservoirs can provide insights

into the processes that are involved in the mobilization of radionuclides in terrestrial ecosystems and help to understand the pathways by which radionuclides are mobilized and transported in the environment.

Acknowledgements Financial support from the CICYT project MEDEROCAR (CGL2008-00831/BTE) is gratefully acknowledged.

References

- Bacon MP, Spencer DW, Brewer PG (1976) $^{210}\text{Pb}/^{226}\text{Ra}$ and $^{210}\text{Po}/^{210}\text{Pb}$ disequilibria in seawater and suspended particulate matter. *Earth Planet Sci Lett* 32:277–296
- Baeza A, Guillén J, Ontalba Salamanca MA, Rodríguez A, Ager FJ (2009) Radiological and multi-element analysis of sediments from the Proserpina reservoir (Spain) dating from Roman times. *J Environ Radioactiv* 100:866–874
- Benninger LK, Lewis DM, Turekian KK (1975) On the use of natural Pb-210 as a heavy metal tracer in the river-estuarine system. In: Church TM (ed) *Marine chemistry in the coastal environment*. American Chemical Society, Washington DC, ACS Symposium Series; chapter 12, vol. 18, pp 202–210
- Callender E, Robbins JA (1993) Transport and accumulation of radionuclides and stable elements in a Missouri River Reservoir. *Water Resour Res* 29:1787–1804
- Chi-Ju L, Yu-Chia C, Tsung-En W (2004) Ra-226 and Pb-210/Ra-226 activity ratio in the Northern South China Sea. In: American Geophysical Union, Spring Meeting 2004, abstract #OS41A-0
- de Jong E, Acton DF, Kozak LM (1994) Naturally occurring gamma-emitting isotopes, radon release and properties of parent materials of Saskatchewan soils. *Can J Soil Sci* 74:47–53
- Dowdall M, O'Dea J (2002) Ra-226/U-238 disequilibrium in an upland organic soil exhibiting elevated natural radioactivity. *J Environ Radioactiv* 59:91–104
- Evans CV, Morton LS, Harbottle G (1997) Pedologic assessment of radionuclide distributions: use of a radio-pedogenic index. *Soil Sci Soc Am J* 61:1440–1449
- Faure G (1986) *Principles of isotope geology*, 2nd edn. Wiley, New York
- Fleischer RL (1983) Theory of alpha recoil effects on radon release and isotopic disequilibrium. *Geochim Cosmochim Acta* 47:779–784
- Foster IDL (2006) Lakes and reservoirs in the sediment delivery system: reconstructing sediment yields. In: Owens PN, Collins AJ (eds) *Soil erosion and sediment redistribution in river catchments*. CAB International, Wallingford, pp 128–142
- Foster IDL, Boardman J, Keay-Bright J (2007) Sediment tracing and environmental history for two small catchments, Karoo Uplands, South Africa. *Geomorphology* 90:126–143
- Fujiyoshi R, Sawamura S (2004) Mesoscale variability of vertical profiles of environmental radionuclides (^{40}K , ^{226}Ra , ^{210}Pb and ^{137}Cs) in temperate forest soils in Germany. *Sci Total Environ* 320:177–188
- Ivanovich M (1994) Uranium series disequilibrium: concepts and applications. *Radiochim Acta* 64:81–94
- Jasinska M, Niewiadomski T, Schwbenthan J (1982) Correlation between soil parameters and natural radioactivity. In: Vohra K, Mishra UC, Pillai KC, Sadasivan S (eds) *Natural radiation environment*. Wiley, New York, pp 206–211
- Jordan C, Cruickshank JG, Higgins AJ, Hamill KP (1997) *The soil geochemical atlas of Northern Ireland*. Department of Agriculture for Northern Ireland, Belfast
- Kabata-Pendias A, Pendias H (2001) *Trace elements in soils and plants*, 3rd edn. CRC, Boca Raton, p. 413
- Krishnaswami S, Somayajulu BLK, Chung Y (1975) $^{210}\text{Pb}/^{226}\text{Ra}$ disequilibrium in the Santa Barbara basin. *Earth Planet Sci Lett* 27:388–392
- Litaor MI (1995) Uranium isotopes distribution in soils at the Rocky Flats Plant, Colorado. *J Environ Qual* 24:314–323
- Lorente A, García-Ruiz JM, Beguería S, Arnaez JM (2002) Factors explaining the spatial distribution of hillslope debris flows. A case study in the Flysch Sector of the Central Spanish Pyrenees. *Mt Res Dev* 22:32–39
- MacKenzie AB (2000) Environmental radioactivity: experience from the 20th century—trends and issues for the 21st century. *Sci Total Environ* 249:313–329
- McCall PL, Robbins JA, Matisoff G (1984) ^{137}Cs and ^{210}Pb transport and geochronologies in urbanized reservoirs with rapidly increasing sedimentation rates. *Chem Geol* 44:33–65
- McLean RI, Summers JK, Olsen CR, Domotor SL, Larsen IL, Wilson H (1991) Sediment accumulation rates in Conowingo reservoir as determined by man-made and natural radionuclides. *Estuaries* 14:148–156
- Megumi K, Oka T, Yaskawa K, Sakanoue M (1982) Contents of natural radioactive nuclides in relation to their surface area. *J Geophys Res* 87:10857–10860
- Mercer TT (1976) The effect of particle size on the escape of recoiling RaB atoms from particulate surfaces. *Health Phys* 31:173–175
- Morellón M, Valero Garcés B, Moreno A, González Sampérez P, Mata P, Romero O, Maestro M, Navas A (2008) Holocene Paleohydrology and climate variability in Northeastern Spain: The sedimentary record of Lake Estanya (Pre-Pyrenean Range). *Quatern Int* 118:15–31
- Navas A, Machín J (2002) Spatial distribution of heavy metals and arsenic in soils of Aragón (NE Spain): controlling factors and environmental implications. *Appl Geochem* 17:961–973
- Navas A, García-Ruiz JM, Machín J, Lasanta T, Walling D, Quine T, Valero B (1997) Aspects of soil erosion in dry farming land in two changing environments of the central Ebro valley, Spain. In: Walling DE, Probst JL (eds) *Human impact on erosion and sedimentation*. IAHS, Wallingford, 245:13–20
- Navas A, Valero-Garcés BL, Machín J (2004) An approach to integrated assessment of reservoir siltation: the Joaquín Costa reservoir as case study. *Hydrol Earth Syst Sci* 8:1193–1199
- Navas A, Machín J, Soto J (2005a) Assessing soil erosion in a Pyrenean mountain catchment using GIS and fallout ^{137}Cs . *Agr Ecosyst Environ* 105:493–506
- Navas A, Soto J, Machín J (2005b) Mobility of natural radionuclides and selected major and trace elements along a soil toposequence in the central Spanish Pyrenees. *Soil Sci* 170:743–757
- Navas A, Valero-Garcés B, Gaspar L, García-Ruiz JM, Beguería S, Machín J, López-Vicente M (2008) Variabilidad espacial del transporte de sedimento en la cuenca superior del río Aragón. *Cuadernos de Investigación Geográfica* 34:39–60
- Navas A, Valero-Garcés BL, Gaspar L, Machín J (2009) Reconstructing the history of sediment accumulation in the Yesa reservoir: an approach for management of mountain reservoirs. *Lake Reserv Manage* 25:15–27
- Navas A, Gaspar L, López-Vicente M, Machín J (2011) Spatial distribution of natural and artificial radionuclides at the catchment scale (South Central Pyrenees). *Radiat Meas* 46:261–269
- Norrisk K (1975) The geochemistry and mineralogy of trace elements. In: Nicholas DJD, Egan AR (eds) *Trace elements in soil plant-animal systems*. Academic, New York, p 55
- Rank D, Kralik M, Gyurits KA, Maringer F, Rajner V, Kurcz I (1987) Investigation of sediment transport in the Austrian part of the Danube using environmental isotopes. *IAEA-SM* 299:637–646
- Schultz LG (1964) Quantitative interpretation of mineralogical composition from X-ray and chemical data of the Pierre Shale. *US Geol Surv Prof Paper* 391C
- Simms AD, Woodroffe C, Jones BG, Hejnis H, Mann RA, Harrison J (2008) Use of ^{210}Pb and ^{137}Cs to simultaneously constrain ages and sources of post-dam sediments in the Cordeaux reservoir, Sydney, Australia. *J Environ Radioactiv* 99:1111–1120
- Sundborg A, Rapp A (1986) Erosion and sedimentation by water: problems and prospects. *Ambio* 15:215–225
- Valero-Garcés BL, Navas A, Machín J, Walling D (1999) Sediment sources and siltation in mountain reservoirs: a case study from the Central Spanish Pyrenees. *Geomorphology* 28:23–41
- Valero-Garcés B, Moreno A, Navas A, Mata P, Machín J, Delgado-Huertas A, González-Sampérez P, Schwab A, Morellón M, Edwards L (2008) The Taravilla lake and Tufa deposits (Central

- Iberian Range, Spain) as paleohydrological and paleoclimatic indicators. *Paleogeogr Palaeocl* 259:136–156
- Vanden Bygaart AJ, Protz R (1995) Gamma radioactivity on a chronosequence, Pinery Provincial Park, Ontario. *Can J Soil Sci* 75:73–84
- Villar L, Sesé JA, Fernández JV (2001) Atlas de la Flora del Pirineo aragonés. II, Instituto de Estudios Altoaragoneses y Consejo de Protección de la Naturaleza de Aragón, Huesca y Zaragoza, p 790
- Walling DE, Owens PN, Foster IDL, Lees JA (2003) Changes in the sediment dynamics of the Ouse and Tweed basins in the UK, over the last 100–150 years. *Hydrol Processes* 17:3245–3269
- Zhang X, Walling DE, Yang Q, He X, Wen Z, Qi Y, Feng M (2006) ^{137}Cs budget during the period of 1960s in a small drainage basin on the Loess Plateau of China. *J Environ Radioactiv* 86:78–91